

Reentrance effect in the lane formation of driven colloids

J. Chakrabarti,¹ J. Dzubiella,^{2,*} and H. Löwen³

¹*S. N. Bose National Centre for Basic Sciences,
Block-JD, Sector-III, Salt Lake, Calcutta - 700091, India*

²*University Chemical Laboratory, Lensfield Road, Cambridge CB2 1EW, United Kingdom*

³*Institut für Theoretische Physik II, Heinrich-Heine-Universität Düsseldorf,
Universitätsstraße 1, D-40225 Düsseldorf, Germany*

(Dated: today)

Recently it has been shown that a strongly interacting colloidal mixture consisting of oppositely driven particles, undergoes a nonequilibrium transition towards lane formation provided the driving strength exceeds a threshold value. We predict here a reentrance effect in lane formation: for fixed high driving force and increasing particle densities, there is first a transition towards lane formation which is followed by another transition back to a state with no lanes. Our result is obtained both by Brownian dynamics computer simulations and by a phenomenological dynamical density functional theory.

PACS numbers: 82.70.-y,61.20.-p,05.40.-a

If a binary colloidal mixture is exposed to a constant external force which acts differently on the two particle species, the system achieves a nonequilibrium steady-state in general [1, 2, 3]. For strong external forces, particles of the same species, which are driven alike, align behind each other [4, 5]. This “slip-stream” effect results in macroscopic lanes spanning the whole system size provided a threshold in the strength of the driving force is exceeded. Lane formation can be classified as a nonequilibrium first-order phase transition. The transition towards lane formation is general and occurs also in systems different from colloids, such as dusty plasma particles [6], ions migrating within two-dimensional membranes [7], granular matter [8, 9], and collective dynamics of pedestrians in pedestrian zones [10].

A quantitative investigation of lane formation has been performed by Brownian dynamics computer simulations of driven two-component colloidal mixture in two and three dimensions [4]. These simulation studies have been extended to asymmetric mixtures [11], relatively tilted driving fields acting on the different particle species [12] and crystalline mixtures driven against each other [12]. Lane formation also occurs as a transient state during the two-dimensional Rayleigh-Taylor interfacial instability provided the interfacial tensions are small with respect to the driving force [13]. Moreover a theory for the transition towards lane formation was recently proposed by us [14]. It is based on dynamical density functional theory, which takes the repulsive interparticle interaction explicitly into account, and is supplemented by a phenomenological version of the transversal particle current induced by the external drive. An instability from a homogeneous state towards a laned state was predicted but the actual predictions for the threshold of the external drive were significantly smaller than in the simulation [4].

The previous studies in Refs. [4, 14] were restricted to high densities of the colloidal particles. In this brief report, we illustrate our observations on the low density regime as well to bring out the entire topology of the laning phase diagram. We show that there is a *reentrant effect* in driven colloidal mixtures. Reentrance occurs as a function of particle density at fixed strength of the external drive. For increasing density and sufficiently high driving force, we find the sequence: no lanes/lanes/no lanes, i.e. lane formation occurs only in a finite density window. There is a simple intuitive reason for this reentrance effect: for very small densities, the particles are almost non-interacting, hence the drive will not induce any instability so that the system will stay mixed for entropy reasons. For intermediate densities, there is an interaction and the strong drive will put particles into lanes. For very high densities, on the other hand, the interaction is very strong exceeding the external drive so that the external drive will again not induce lane formation. Our results are based on Brownian dynamics computer simulations. We also adopt the dynamical density functional theory of Ref. [14]. However, we improve the phenomenological expression for the transverse current in this theory and show that the modified theory captures the reentrant feature and brings about much better agreement with the simulation data for the location of the laning transition.

The Brownian dynamics simulation model in this work is the same as used in our previous studies [4, 14]. Let us briefly summarize the essential features: we consider an equimolar binary colloidal system with $2N = 500$ particles in a square cell of length ℓ , having periodic boundary conditions with a fixed total number density $\rho_0 = 2N/\ell^2 = 2\rho_+^0 = 2\rho_-^0$ and a fixed temperature T . The effective pair potential between two colloidal particles at a separation r is modeled as a screened Coulomb interaction [2]

$$V(r) = V_0 \sigma \exp[-\kappa(r - \sigma)/\sigma] / r, \quad (1)$$

where V_0 is an energy scale, σ is the length scale, defining

*e-mail address: jd319@cam.ac.uk

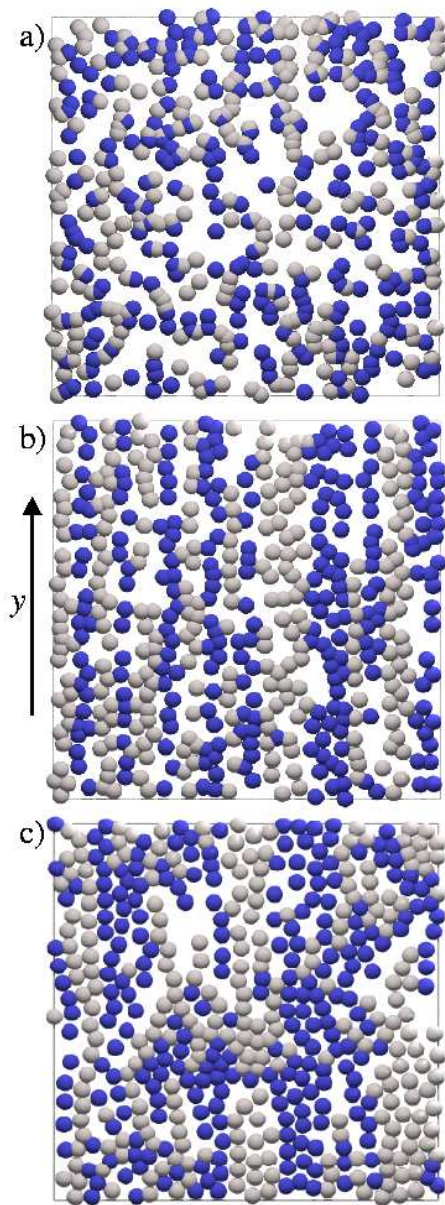


FIG. 1: Simulation snapshots for a fixed external force $F^* = 70$ and for densities (a) $\rho_0\sigma^2 = 0.07$, (b) $\rho_0\sigma^2 = 0.20$, and (c) $\rho_0\sigma^2 = 0.70$. The driving force is acting in y -direction as indicated by the arrow. The particle and box sizes in this figure are scaled to the same lengths for a better comparison of the structure.

the range of the interaction, and κ the reduced inverse screening length. In this work the energy is chosen to be $V_0 = 10k_B T$, where $k_B T$ is the thermal energy, and $\kappa = 4.0$. The parameters are the same for the interaction between particles of both types, and also for the cross interaction. The dynamics of the colloids is completely overdamped Brownian motion. We neglect hydrodynamic interactions which is justified for small colloidal

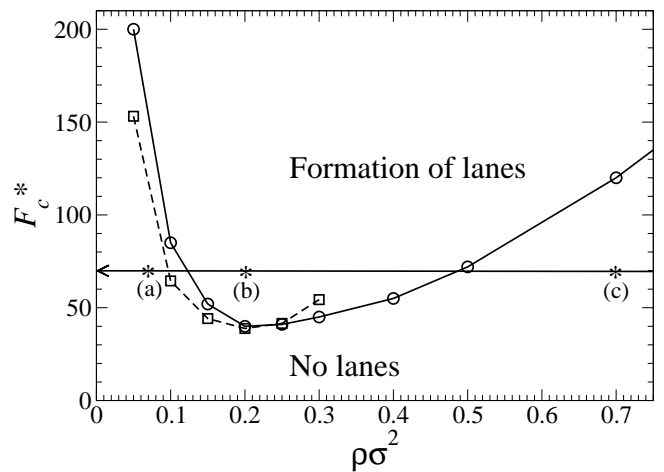


FIG. 2: The critical force F_c for lane formation versus density ρ_0 . Brownian dynamics simulation results (circles) are compared to the dynamic density functional theory (squares). Solid and dashed lines are guide to the eye and suggest the phase boundary between states of 'no lanes' and 'lane formation'. The asterisks mark states of chosen densities (a) $\rho_0\sigma^2 = 0.07$, (b) $\rho_0\sigma^2 = 0.20$, and (c) $\rho_0\sigma^2 = 0.70$ and a fixed force $F^* = 70$ (indicated by the arrow), for which snapshots are shown in Fig. 1.

volume fractions and long-ranged colloidal pair interactions. The constant external field F_i ($i = +, -$) is acting in y -direction of the simulation cell, shown in Fig.1, and drives particles of different types in opposite directions: $F_+ = F > 0$ for (+) particles and $F_- = -F$ for (-) particles. We denote the dimensionless drive parameter by $F^* = F\sigma/k_B T$. In order to detect lane formation we apply the order parameter ϕ which is defined in [4]. It is zero, when the system is isotropic, and one, when the colloids are perfectly ordered in lanes throughout the whole system, each lane containing only particles of the same type. We could show in [4], that ϕ , averaged over many steady-state configurations, increases rapidly to values of about one when critical threshold value of the applied field, F_c is exceeded, indicating a nonequilibrium phase transition to the laning state. We define F_c to be the external field for which $\phi = 0.5$, implying that in average half of the particles in the system are ordered in well defined lanes. Results for the critical force F_c versus the total density are plotted in Fig. 2, showing a nonmonotonic behavior: for fixed high driving force (for instance $F^* = 70$ as indicated by an arrow in Fig. 2) and increasing particle densities, there is first a transition towards lane formation which is followed by another transition back to a state with no lanes. Corresponding snapshots for the three states at three different densities $\rho_0\sigma^2 = 0.07, 0.20, 0.70$ for a fixed force $F^* = 70$ are shown in Fig. 1(a)-(c). The average order parameter for these parameters is $\phi = 0.11, 0.80, 0.05$, respectively. At the highest density (Fig. 1(c)), there a still remnant of

laning visible but there are also regions of mutual jamming which destroy perfect lane formation. Hence there are qualitative differences in the no-lane phase at small and high densities.

A dynamical density functional theory as described in Ref. [14] accounts for the stabilization of the inhomogeneous steady states beyond the critical drive. The density fields $\rho_{\pm}(\vec{r}, t)$ obey the equation of motion which has the form of continuity equation:

$$\frac{\partial \rho_{\pm}(\vec{r}, t)}{\partial t} = -\nabla \cdot [\vec{j}_{\pm}^{(1)}(\vec{r}, t) + \vec{j}_{\pm}^{(2)}(\vec{r}, t) + \vec{j}_{\pm}^{(3)}(\vec{r}, t)]. \quad (2)$$

The first current term $\vec{j}_{\pm}^{(1)}(\vec{r}, t)$ is a diffusive current, and modeled as [14, 15]:

$$\vec{j}_{\pm}^{(1)}(\vec{r}, t) = -\frac{D}{k_B T} \rho_{\pm}(\vec{r}, t) \nabla \frac{\delta \mathcal{F}[\rho_+, \rho_-]}{\delta \rho_{\pm}(\vec{r}, t)}, \quad (3)$$

$D = k_B T / \gamma$ being the phenomenological diffusion coefficient. $\mathcal{F}[\rho_+, \rho_-]$, the free energy cost for creating weak inhomogeneities around a homogeneous state, is given by [16]:

$$\begin{aligned} \frac{\mathcal{F}[\rho_+, \rho_-]}{k_B T} &= \sum_{k=\pm} \int d^2 r \rho_k(\vec{r}) \log[2\rho_k(\vec{r})/\rho_0] \\ &- \frac{1}{2} \int d^2 r d^2 r' c(|\vec{r} - \vec{r}'|) \Delta \rho(\vec{r}) \Delta \rho(\vec{r}') \end{aligned} \quad (4)$$

with $\Delta \rho(\vec{r}) = \rho_+(\vec{r}) + \rho_-(\vec{r}) - \rho_0$ and $c(r)$ the fluid direct correlation function, determined by $V(r)$ [16]. $\vec{j}_{\pm}^{(2)}(\vec{r}, t)$, is induced by the driving field in y direction. In a completely demixed state, the field induces a Brownian drift velocity of $v_d = F/\gamma$ in the y direction, while in a completely mixed state the flow is reduced due to mutual collisions between oppositely driven particle. These effects can be incorporated via:

$$\begin{aligned} \vec{j}_{\pm}^{(2)}(\vec{r}, t) &= \mp \vec{e}_y \frac{2v_d}{\rho_0} [1 + \alpha \rho_{\pm}(\vec{r}, t) (\rho_0/2 \\ &- \rho_{\pm}(\vec{r}, t)) - \beta \rho_+(r, t) \rho_-(r, t)], \end{aligned} \quad (5)$$

where α is a phenomenological parameter to take care of the appropriate physical dimensions of the current and β takes care of the mutual collision effects. $\vec{j}_{\pm}^{(3)}(\vec{r}, t)$ is also induced by the external drive but in the x direction transverse to the drive. Brownian collisions between $+$ and $-$ particles having repulsive interaction will cause a displacement perpendicular to the field. The leading term contributing to $\vec{j}_{\pm}^{(3)}(\vec{r}, t)$ is the gradient in the density difference field [14]. $\vec{j}_{\pm}^{(3)}(\vec{r}, t)$ should scale with the total collision cross-section experienced per unit time. Let σ_0 denote a typical range of the interaction $V(r)$ needed to perform a collision and $a_s = \rho_0^{-1/2}$ the mean interparticle separation. The number of collision event will be given by the number of particles of the two species in an area of $a_s \sigma_0$. The typical time of collision is a_s / v_d , so that the number of collision per unit

time is $\frac{v_d}{a_s} \rho_+(\vec{r}, t)(0) \rho_-(\vec{r}, t) (a_s \sigma_0)^2$. The cross-section of an individual collision is given by $\pi \sigma_0^2 / 2$, where the factor of half takes care of the fact that the scattering is anisotropic due to the drive, only half portion of a particle being exposed to collision. Consequently we find

$$\begin{aligned} \vec{j}_{\pm}^{(3)}(\vec{r}, t) &= \pm \vec{e}_x \pi \sigma_0^2 / 2 \frac{v_d}{a_s} \rho_+(\vec{r}, t)(0) \rho_-(\vec{r}, t) (a_s \sigma_0)^2 \\ &\times \frac{\partial}{\partial x} [\rho_+(\vec{r}, t) - \rho_-(\vec{r}, t)]. \end{aligned} \quad (6)$$

All currents remain unchanged under the interchange of the species, namely, $\rho_+(\vec{r}, t) \leftrightarrow \rho_-(\vec{r}, t)$ and $F \rightarrow -F$, which satisfies the symmetry requirement. σ_0 has been estimated by an effective hard core diameter from the Barker-Henderson perturbation theory, $\sigma_0 = \int_0^\infty [1 - \exp(-V(r)/k_B T)] dr$.

The dispersion relations for frequency ω with wave vector $\vec{q} = (q_x, q_y)$, obtained from the linearized equations of motion [14] show that real frequencies, as required for the steady state bifurcations, can result for $q_y = 0$, independent of α and β . The unstable wave vector in the y direction being $q_y = 0$ indicate structural homogeneity in the y -direction parallel to the drive as observed in the simulations. Two possible dispersion relations for $q_y = 0$ are:

$$\omega_1^* = 2F^* q_x^2 - [1 - \rho_0 \tilde{c}(q_x, q_y = 0)] q_x^2 \quad (7)$$

and

$$\omega_2^* = -[1 - \rho_0 \tilde{c}(q_x, q_y = 0)] q_x^2, \quad (8)$$

where $\omega_{1,2}^* = \omega_{1,2} \sigma_0^2 / D$ denotes the dimensionless frequency and $\tilde{c}(\vec{q})$ is the Fourier transform of $c(r)$. ω_2^* remains negative for all q_x , since $1 - \rho_0 \tilde{c}(\vec{q})$, being the inverse of the static structure factor, is a positive definite quantity [16]. ω_1^* changes sign, indicating the steady state bifurcation of a homogeneous state to an inhomogeneous state [17]. q_0 where ω_1^* has a positive maximum as a function of q_x , will dominate the growth of the inhomogeneous phase. We approximate $c(r)$ by that of an effective hard disk fluid with effective diameter σ_0 for which analytical expressions are known [18]. We calculate numerically ω_1^* and locate graphically the instability point as well as q_0 [14]. For a given ρ_0 ω_1^* remains negative for all q_x indicating the stability of the homogeneous phase for very low F^* . The homogeneous phase becomes unstable for $F^* > F_c$ to density perturbations with q_x over a band about the maximum at $q_x = q_0$. Note that a state with density modes having $q_y = 0$ but a finite $q_x = q_0$ indicates a lane phase as observed in the steady states of the BD simulations. The stability of the different phases has been shown over the F^* -vs- ρ_0 plane in Fig. 2, F_c^* being marked by the squares for chosen densities.. The most striking feature of the stability diagram is the reentrant homogeneous phase as one increases the density for a fixed external force. Physically, the diffusive thermodynamic current tries to avoid any $+/-$ interface via entropy of mixing, while the current

$\vec{j}_{\pm}^{(3)}(\vec{r}, t)$ amplifies particle segregation in x direction via collisions induced by the drive. The diffusion becomes slower with increasing ρ_0 that reduces the tendency of mixing. This requires stronger drive to ensure the collision between two different species to have an appreciable $\vec{j}_{\pm}^{(3)}(\vec{r}, t)$ contribution. This is what seen in the large ρ_0 regime where F_c increases with ρ_0 . However, the collision frequency itself goes down in the low ρ_0 regime, and one needs stronger drive to counterbalance the fast diffusing current, leading to the reentrant behavior seen in Fig. 2.

In conclusion, we predict a reentrance effect in binary mixtures of oppositely driven colloids for increasing density. At fixed driving strength, there is a state with no lanes at small densities. This transforms into a state with lanes for intermediate densities and then there is reentrance of the state with no lanes. The reentrance behavior has a simple intuitive interpretation and should therefore be robust with respect to a variation of details of the interaction. We expect that it will show up also for asymmetric mixtures, in three spatial dimensions, and for different particle dynamics than the simple Brownian dynamics assumed in our model. In fact, recent simulations [19] which include hydrodynamic interactions have revealed that the laning transition itself is indeed stable

when explicit hydrodynamic interactions are added.

The reentrance behavior should be verifiable in experiments. We think that the most promising candidate for an experimental test are binary mixtures of highly charged colloidal suspensions in a gravitational field. Recent progress has been made which highly deionized suspensions [20] which can be subject to sedimentation at different colloidal densities. Another possibility are mixtures of colloids and polymers under gravity [21]. The reentrance effect may finally provide also a quantitative framework to explain different states of pedestrian dynamics in pedestrian zones for varied population density [22]: The low-density state without lanes is typical for low populations. For intermediate densities, pedestrians form lanes, but for even higher densities the lanes are broken again and there is a crossover to panic dynamics.

Acknowledgments

We thank H. K. Janssen for helpful discussions and the DFG for support within the SFB TR6. J.D. acknowledges the financial support from the EPSRC within the Portfolio Grant RG37352.

-
- [1] H. Löwen, *J. Phys.: Condensed Matter* **13**, R415 (2001).
 - [2] P. N. Pusey, in *Liquids, Freezing and the Glass Transition*, edited by J. P. Hansen *et al.* (North Holland, Amsterdam, 1991).
 - [3] J. K. G. Dhont, *An Introduction to Dynamics of Colloids* (Elsevier, Amsterdam, 1996).
 - [4] J. Dzubiella, G. Hoffmann, and H. Löwen, *Phys. Rev. E* **65**, 021402 (2002).
 - [5] J. Dzubiella, H. Löwen, and C. N. Likos, *Phys. Rev. Lett* **91**, 248301 (2003).
 - [6] H. M. Thomas, D. D. Goldbeck, T. Hagl, A. V. Ivlev, U. Konopka, G. E. Morfill, H. Rothermel, R. Sutterlin, M. Zuzic, *Physica Scripta* **T89**, 16 (2001).
 - [7] R. R. Netz, *Europhys. Letters* **63**, 616 (2003).
 - [8] P. Valiveti and D. L. Koch, *Physics of Fluids* **11**, 3283 (1999).
 - [9] S. B. Santra *et al.*, *Phys. Rev. E* **54**, 5066 (1996).
 - [10] D. Helbing *et al.*, *Environment and Planning B: Planning and Design* **28**, 361 (2001).
 - [11] H. Löwen, J. Dzubiella, *Faraday Discussions* **123**, 99 (2003).
 - [12] J. Dzubiella, H. Löwen, *J. Phys.: Condensed Matter* **14**, 9383 (2002).
 - [13] A. Wysocki, H. Löwen, cond-mat 0402318
 - [14] J. Chakrabarti, J. Dzubiella, H. Löwen, *Europhys. Letters* **61**, 415 (2003).
 - [15] P. M. Chaikin and T. C. Lubensky, *Principles of Condensed Matter Physics* (Cambridge University Press, Cambridge, 1995).
 - [16] J. P. Hansen and I. R. McDonald, *Theory of Simple Liquids*, 2 ed. (Academic Press, London, 1986).
 - [17] G. Nicolis and I. Prigogine, *Self-organization in Nonequilibrium Chemical Systems* (Springer-Verlag, Berlin, 1977).
 - [18] M. Baus and J.-L. Colot, *Phys. Rev. A* **36**, 3912 (1987).
 - [19] J. Padding, A. A. Louis, private communication, to be published.
 - [20] C. P. Royall, M. E. Leunissen, A. van Blaaderen, *J. Phys.: Condensed Matter* **15**, S3581 (2003).
 - [21] D. G. A. L. Aarts, J. H. van der Wiel, H. N. W. Lekkerkerker, *J. Phys.: Condensed Matter* **15** S245 (2003).
 - [22] D. Helbing, I. J. Farkás, P. Molnár, T. Vicsek, "Simulation of pedestrian crowds in normal and evacuation situations", in *Pedestrian and Evacuation Dynamics*, M. Schreckenberg and S. D. Sharma (eds.), pages 21-58, Springer, Berlin (2002).